Article

Numerical Modelling of the Mulino Delle Vene Aquifer (Northern Italy) as a Tool for Predicting the Hydrogeological System Behavior under Different Recharge Conditions

Francesca Petronici [1], **Estanislao Pujades** [2,*], **Anna Jurado** [3], **Marco Marcaccio** [4] **and Lisa Borgatti** [1]

[1] DICAM, Department of Civil, Chemical, Environmental and Materials Engineering, Alma Mater Studiorum University of Bologna, Viale Risorgimento, 2, 40136 Bologna, Italy; francesca.petronici2@gmail.com (F.P.); lisa.borgatti@unibo.it (L.B.)

[2] Department of Computational Hydrosystems, UFZ–Helmholtz Centre for Environmental Research, 04318 Leipzig, Germany

[3] Institute for Groundwater Management, Technische Universität Dresden, 01062 Dresden, Germany; anna.jurado@tu-dresden.de

[4] Arpae Emilia-Romagna, 40122 Bologna, Italy; mmarcaccio@arpae.it

* Correspondence: estanislao.pujades-garnes@ufz.de or estanislao.pujades@gmail.com; Tel.: +49-341-235-1784

check for updates

Abstract: Water scarcity periods will increase in frequency and magnitude in the near future, especially in Mediterranean regions, and proper groundwater management has been recognized as a key issue to mitigate possible impacts. In this context, numerical models acquire a special relevance to quantify the availability of water resources and predict their behavior under changing climate conditions. This work shows the procedure followed to model a mountainous fractured aquifer located in the northern Apennines (Italy) using an open source code. This aquifer feeds springs with an average discharge of about 96.8 L/s. Even though they are not exploited at the moment, these springs might represent a relevant resource of freshwater for public water supply and are essential for ecosystem sustainment. The main limitation faced to model the aquifer in a realistic way is the lack of data, which hinders the calibration of the model. A nonconventional procedure was followed to obtain information on the hydraulic parameters. The hydraulic conductivity is computed from a steady-state calibration for which a limited number of groundwater head observations are available, whilst information concerning the storage coefficient is obtained analytically from the spring discharge recession curve. Finally, the model is used for predicting the system behavior under different groundwater recharge scenarios. Numerical simulations and analytical approximations reveal that the studied aquifer can provide fresh water under different groundwater recharge conditions and has the capacity to smooth the effects of short drought periods, representing an option for water management strategies in the region.

Keywords: groundwater; numerical modelling; recession curve; water management; northern Apennines; Italy

1. Introduction

Pressure on freshwater resources has increased in the last decades due to the rapid population growth coupled with intense anthropogenic activities (i.e., agricultural and industrial processes and/or high urban water supply demand). In fact, the global water demand has increased 35 fold in the

last 330 years [1]. Moreover, the last Intergovernmental Panel on Climate Change reports [2,3] have asserted that climate change will affect the quantity and quality of water resources in many regions. In particular, groundwater bodies will be affected by changes in groundwater recharge and by the increment of irrigation demand [4], which will altogether contribute to the progressive drying of aquifers. In this context, it is of paramount importance to foresee the effects of climate change and water demand on groundwater in order to properly manage this valuable resource and face possible future drought periods [5,6].

Changes to groundwater recharge and irrigation will be especially relevant in regions where groundwater resources are widely used, like in Italy. According to ISTAT [7], 85.5% of drinking water comes from groundwater (35.7% from springs and 49.8% from wells). Therefore, prolonged drought periods may reduce the availability of drinking water. In this context, a proper management practice of water resources is fundamental. To mitigate the impact of droughts, a comprehensive analysis and a conscious use of groundwater resources are needed [8]. Italian mountainous watersheds are important sources of water for local and downstream ecosystems and human populations. Consequently, a sound water management approach must be developed also in these basins, which requires an in-depth investigation of the hydrogeological processes. Several authors have evaluated the effects of climate change on Italian groundwater resources. Cambi and Dragoni [9] carried out the first attempt to assess the effects of climate change on the Bagnara spring (central Italy). A higher decrease of spring discharge with respect to the decrease of the recharge was found, highlighting the vulnerability of groundwater sources at this particular site. Later, this result was confirmed by Dragoni et al. [10]. Similarly, Gattinoni and Francani [11] assessed the effects of different groundwater recharge conditions on the depletion curve of the fractured system of the Nossana spring (northern Italy) and Dragoni et al. [12] developed a numerical model of the Scirca spring in the central Apennines, which is fed by a fractured limestone massif, to test the efficiency of various management schemes on the water resources. In the same line, Liuzzo et al. [13] investigated different groundwater recharge conditions in Sicily, showing a worsening of water stress due to a negative trend in precipitation and an increase in evapotranspiration. Finally, Vezzoli et al. [14] analyzed the effects of climate change scenarios on the Po River discharge with a hydrological model. During summer, they forecasted a reduction in precipitation leading to an increase in low flow duration. Conversely, the frequency of the high flows is expected to increase in autumn and winter when precipitation shows a positive variation. To sum up, during the last years some studies have been carried out on the impacts of climate change on groundwater in Italy. However, little attention has been paid to the northern Apennines water resources. This is likely due to the small volumes of mountainous aquifers compared to major aquifers located in the alluvial plain sediments [15]. However, mountainous aquifers represent a valuable source of water in some regions for public supply and to sustain the ecosystem [16].

The objective of this work is to provide a methodology for estimating the impacts of changes in groundwater recharge on groundwater resources in an area of the northern Apennines by means of numerical modelling. The study area is located within the Tresinaro stream catchment in the northern Apennines (Italy), focusing on its main groundwater source, the Mulino delle Vene springs (420 m a.s.l., Carpineti, Reggio Emilia province, Figure 1). A number of tracer tests carried out during the low flow period along the Tresinaro stream in 2015 highlighted that no other major source of groundwater can be found downstream of the Mulino delle Vene springs [16]. This reveals that a decrease of springs' discharge could lead to a decrease of stream flow, affecting both the stream ecosystem and the drinking water supply from the wells drilled in the downstream alluvial plain. Furthermore, it is likely that the impacts could be similar in all the northern Apennines basins. In fact, the northern Apennines are characterized by the presence of hundreds of springs whose discharge is lower than a few L/s during low flow periods and that renew the groundwater stored within the aquifer almost completely every hydrological year [17]. These hydrogeological characteristics make water resource management in the area quite difficult, especially during the dry season, when an increase of potable water consumption

associated with tourism also occurs. Thus, it is important to assess the possible effects of changes in the groundwater recharge on the springs' discharge.
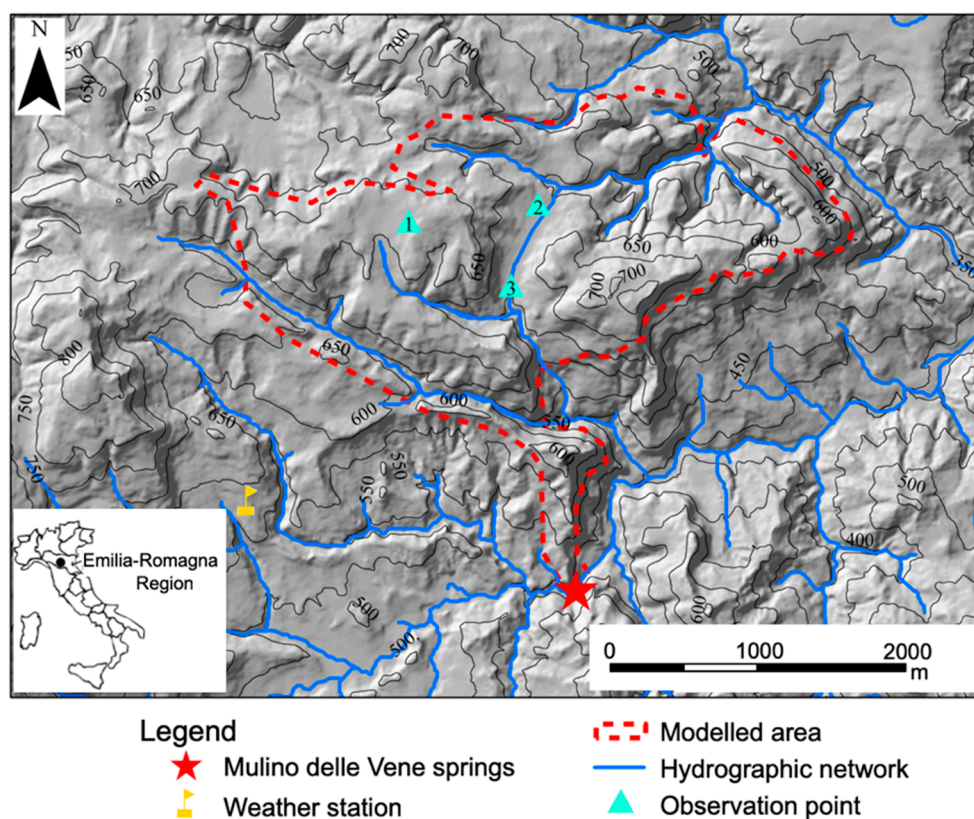

Figure 1. Geographical setting of the study area. The modelled area has an extension of 5.73 km^2. The Mulino delle Vene springs outflow in the Tresinaro stream. The Carpineti weather station is also reported, along with the groundwater observation points (wells and surface water bodies).

In this context, a comprehensive hydrogeological investigation was carried out and the effect of changing groundwater recharge conditions on the piezometric head distribution and spring discharge was assessed. The results of this analysis can be used by stakeholders in the development of a proper management practice of the water resource in the area and to prevent, or at least mitigate, the effects of future water scarcity periods.

2. Materials and Methods

2.1. Conceptual Site Model

2.1.1. General Description of the Study Area

The object of this study is the Mulino delle Vene springs, located in the northern Apennines (Reggio Emilia Province, Italy), at an elevation of 420 m a.s.l. The springs feed the Tresinaro stream, originating in the municipality of Carpineti (562 m a.s.l.) and then flowing for 47 km until Rubiera (53 m a.s.l.), where it joins the river Secchia (tributary of the Po River). The Tresinaro stream hydrological catchment covers approximately an area of 147 km^2, while the recharge area of the aquifer (5.5 km^2, mean altitude of 620 m a.s.l., [18]; Figure 1) extends across a gentle slope in a non-urbanized area. In particular, with reference to 2008 data [19], the agricultural lands are 41% of the springs recharge area, the forest is 58%, and the urban lands are 1%. The mountainous part of the catchment, in fact, is scarcely urbanized, with a population density of 45.7 people per km^2 at Carpineti, 44.9 people per km^2 at Baiso, and 75.7 people per km^2 at Viano [20].

The Mulino delle Vene springs belong to the so-called M Fuso-Castelnovo Monti–Carpineti mountain aquifer, from which a total of 4×10^5 m^3/year are withdrawn by springs exploited for public water supply, and 1×10^5 m^3/year by wells for other purposes. The groundwater from Mulino delle Vene springs is not exploited at present. In the Reggio Emilia Province, average water consumption is 178 L/person/day (2010), which represents the lowest consumption in the whole Emilia-Romagna Region (217 L/person/day). In general, water consumption in the study area has progressively decreased in the last 40 years, from 1975 to 2010 [21].

In large areas of the northern Apennines, a number of low-yield springs fed by unconfined fractured aquifers provide water for drinking and industrial purposes. These aquifers generally display relatively superficial and short groundwater flow paths within the fractured sedimentary rock units, renewing the stored groundwater almost completely every hydrological year [17]. This hydrogeological setting results in discharges that follow rain and snow recharge, with low-flow periods concentrated in summer until early autumn. Therefore, the springs are sensitive to climatic conditions. In 2003 and 2017, in fact, prolonged drought periods resulted in water shortage during summer, when consumption of drinking water increases due to seasonal tourism, and water was being delivered with trucks [22].

2.1.2. Climate

As far as climate of the area is concerned, temporal trend analysis by Antolini et al. [23] highlights a general increase in annual mean temperature and a general decrease in annual cumulated precipitation for the period 1931–2010, associated with an amplification of the seasonal cycle. In particular, data shows a significant increase in mean annual temperatures all over the region (about +0.5 °C/decade). Precipitation shows a less clear behavior with both local decrease and increase (e.g., −100 mm/decade over the western mountains; increase in some areas close to the Po River Delta). A previous study by Cervi et al. [22] based on downscaled regional climate models (RCM) showed an increase of mean annual temperatures (of about +1.3 °C) and an almost steady mean annual precipitation in future periods (2021–2050) with respect to the baseline (1984–2013). These results are similar to those found by Tomozeiu et al. [24] and Dubrovský et al. [25] for the Northern Apennines in general.

Locally, rainfall and air temperature data collected at the weather station of Carpineti (Figure 1) from 2004 to 2014 have been analyzed by Cervi et al. [22]. The average cumulative annual rainfall is about 887 mm, ranging between 489 and 1274 mm, and two main wet seasons occur in March–April and October–November. The average annual temperature is about 12.7 °C. The hottest month is July with an average temperature about 22.7 °C, while the coldest month is January with an average of 3.3 °C. The average effective rainfall (i.e., the part of precipitation that remains at the ground surface after evaporation and transpiration processes and is thus available for subsequent infiltration and runoff) has been assessed on a daily time scale as the difference between the rainfall and the computed evapotranspiration with the Hargreaves formula [26], as suggested by Allen et al. [27]. This assumption is acceptable since the lack of runoff in the streambeds during the whole year suggests that almost all meteoric water can be considered as recharging the aquifer [18]. Moreover, the amount of abstractions is negligible since the area is sparsely urbanized and no industrial facilities can be found. The average effective rainfall is 1.6 mm/day (584 mm/year, 65.8% of the average annual rainfall [16]), which is coherent with literature [28–30]. This value is slightly higher (about 100 mm/year) than the one assessed by Cervi et al. [22] using the Thornthwaite and Mather equation [31]. This is probably due to the different time scale of the two methods (monthly vs. daily average).

2.1.3. Geology of the Study Site

In the study area, Epiligurian and Ligurian geological units outcrop [32] (Figure 2). In particular, the Cigarello formation (CIG), constituted by clay-shales, crops out in the uppermost part of the basin. The Tresinaro stream (Figures 2 and 3) crosses some outcrops of the Pantano formation (PAT), which is subdivided in different sub-units according to the ratio of arenitic to pelitic layers (A/P ratio). Among

these, the unit of Santa Maria (PAT4) has the higher A/P ratio. In the upper part of the stream path, the Contignaco (CTG) and the Antognola (ANT) formations can be found, which are mainly marly rock masses. In the middle part of the basin, clay rich units are outcropping (AVI, Clay of Viano; APA, Palombini shale; AVV, Varicolori clays) together with flysch rock masses (BAI, Brecce Argillose of Baiso; SCB, Scabiazza sandstones). Then, it is possible to find the Ranzano formation (RAN) constituted mainly by sandstones and the Monte Cassio Flysch (MCS).
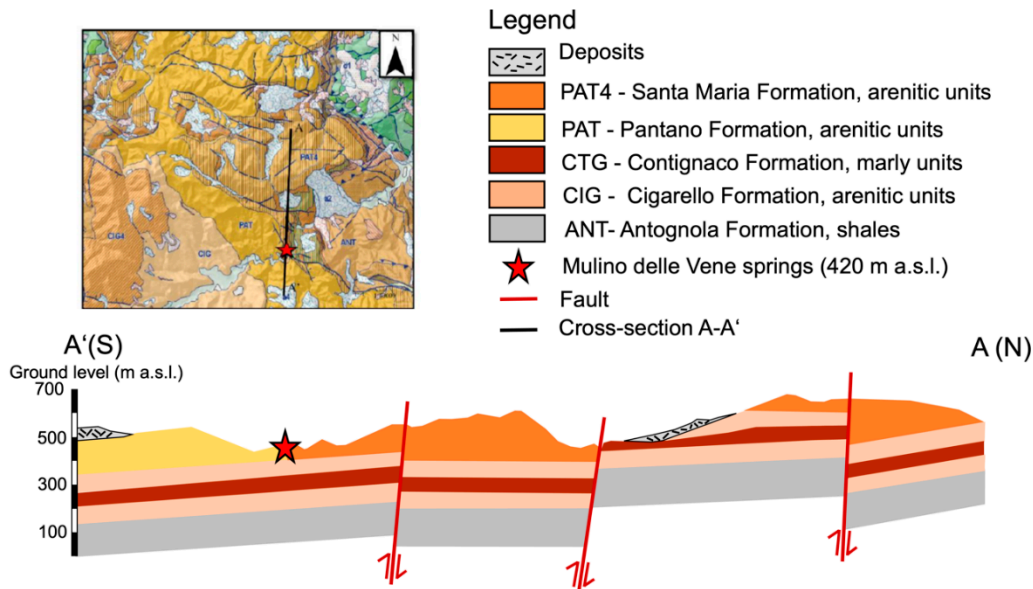

Figure 2. Geological map of the Mulino delle Vene springs area (from Foglio 2018 Castelnovo ne' Monti), (**top**) and cross-section [33] (**bottom**).

The Mulino delle Vene springs originate at the bottom of a 50 m-long hillside, on the left slope of the Tresinaro stream valley (Figure 2). This hillside represents the southern termination of a continuous and poorly deformed sandstone plateau (made up by Santa Maria sandstones, PAT4) bounded by high-angle normal faults, overlying almost impermeable marls (Contignaco Marls, CTG). These faults have strongly affected PAT4 rock mass conditions. The most evident discontinuity has in fact generated the relatively deep Rio Fontanello valley (Figure 2). The bedding of the PAT4 plateau is gently dipping towards the southeast (see the geological cross-section Figure 2), facilitating the groundwater flow towards the Mulino delle Vene springs. These springs represent the final source point of the hydrogeological system. Based on Cervi et al. [18], it is possible to affirm that the main aquifer feeding the springs is the fractured sandstones unit (PAT4). The size of the recharge area is approximately 5.5 km^2 and it extends along a gentle slope in a non-urbanized area [22].
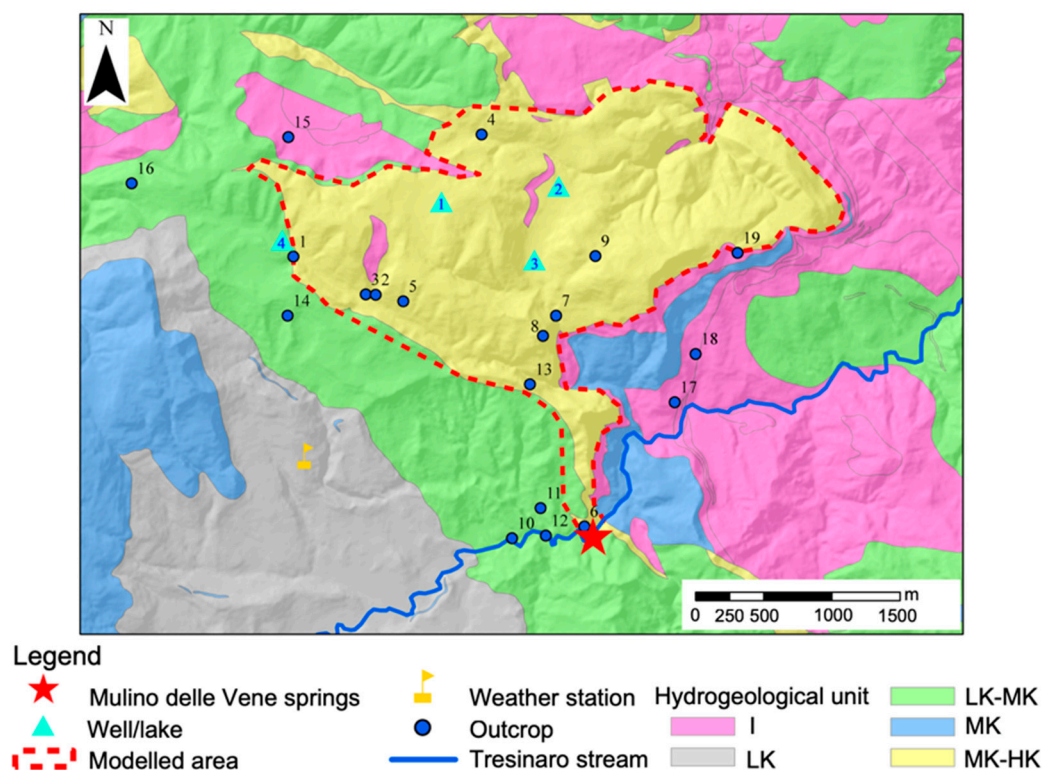
Figure 3. Map of the main hydrogeological units in the Mulino delle Vene springs area. The Mulino delle Vene springs outflow in the Tresinaro stream. The Carpineti weather station is also reported, along with the groundwater observation points (wells and surface water bodies). The blue dots represent the outcrops where the geo-structural and geo-mechanical surveys have been carried out.

2.1.4. Hydrogeology of the Study Site

The geological units outcropping in the area were grouped in hydrogeological structures (Figure 3, [34]). In particular, the following hydrogeological units were defined:

- MK-HK, Medium conductivity ($10^{-6} < k < 10^{-2}$ m/s)-High conductivity ($k > 10^{-2}$ m/s) unit constituted by the S. Maria sandstone (PAT4);
- MK, Medium conductivity ($10^{-6} < k < 10^{-2}$ m/s) unit gathering the Cigarello sandstones (CIG4) and the Contignaco (CTG) formation;
- LK-MK, Low conductivity ($10^{-9} < k < 10^{-6}$ m/s)-Medium conductivity ($10^{-2} < k < 10^{-6}$ m/s) unit grouping the Pantano (PAT), the Scabiazza sandstones (SCB), and the Ranzano formation (RAN);
- LK, Low conductivity ($10^{-9} < k < 10^{-6}$ m/s) unit constituted by the pelites of the Cigarello formation (CIG);
- I, Impermeable ($k < 10^{-9}$ m/s) unit grouping the Antognola formation (ANT) and the shales.

Previous works focused on the region have evaluated *K* using different methods. At first, *K* has been assessed using the fluid-flow theory [35] based on geo-structural data collected in the field along scanlines on 19 outcrops (blue dots in Figure 3) [36–38]. Field surveys have consisted of collecting data along scanlines on different rock outcrops with compass and clinometer. According to the ISRM recommendations, joint spacing, aperture, and persistence have been measured along with hydraulic and joint strength conditions (roughness, wall strength, degree of alteration, filling materials). Based on these data, the hydraulic conductivity of the outcropping geological units has been calculated. The calculated value of *K* at the different locations is specified in Table 1. Assessed *K* in PAT4 outcrops ranges from 10^{-4} to 2.7×10^{-2} m/s (average value equal to 6.1×10^{-3} m/s), whereas it ranges from 9.1×10^{-5} to 4.4×10^{-4} m/s (average value equal to 2.1×10^{-4} m/s) in PAT outcrops. A pumping

test has been also undertaken using a pumping well screened across PAT units (well number 4 in Figure 3) [16]. The result of this test revealed a K of 5×10^{-7} m/s [16] for PAT materials, which differs from the results obtained for outcrops.

Table 1. Values of hydraulic conductivity (K, m/s) assessed in outcrops (Figure 3).

Outcrop	Unit	K (m/s)	Hydrogeological Classification
1	PAT 4	2.7×10^{-2}	HK
2	PAT 4	1.9×10^{-4}	MK
3	PAT 4	1.1×10^{-3}	MK
4	PAT 4	9.3×10^{-4}	MK
5	PAT 4	1.0×10^{-4}	MK
6	PAT 4	5.5×10^{-3}	MK
7	PAT 4	8.0×10^{-3}	MK
8	PAT 4	1.1×10^{-2}	HK
9	PAT 4	8.2×10^{-3}	MK
10	PAT	closed fractures	I
11	PAT	1.1×10^{-4}	MK
12	PAT	4.4×10^{-4}	MK
13	PAT 4	2.8×10^{-4}	MK
14	PAT	9.1×10^{-5}	MK
15	CTG	7.8×10^{-3}	MK
16	PAT 4	5.8×10^{-3}	MK
17	CTG	6.0×10^{-4}	MK
18	CTG	closed fractures	I
19	CTG	3.7×10^{-3}	MK
Well 4	PAT	5×10^{-7}	LK

The values of K obtained in previous works were used as initial parameters for the calibration of the numerical model and to verify the calibration results. In addition, these previous works allow deducing some features of the system, useful to define the boundary conditions of the model. The contrast between the calculated K for PAT units, using a pumping test, and that obtained for PAT4 materials, by geo-structural surveys, indicates that the groundwater exchange between PAT4 and the surrounding materials (PAT and clay-rich units) is very low. Thus, a no-flow boundary condition can be used along the PAT4 boundary.

As far as groundwater level is concerned, two water wells were available in the study area (points 1–2 in Figures 1 and 3). Further data was also obtained from the hydraulic head in a small lake (point 3 in Figures 1 and 3). The first well (point 1 in Figures 1 and 3) is located in the upper part of a hill (712 m a.s.l.) and it is drilled across the PAT4 unit. The second well and the lake (points 2–3 in Figures 1 and 3) are located on alluvial deposits (Figure 2), at the bottom of a valley, at 608 and 601 m a.s.l., respectively. The observation points were monitored three times during the autumn of 2013 (Table 2).

Table 2. Measured piezometric head in the observation points.

Observation Point	Location	Elevation (m a.s.l.)	Observed Piezometric Head (m a.s.l.)			Average Piezometric Head (m a.s.l.)
			25.09.13.	05.11.13.	26.11.13.	
1	Valcava	712	704.3	704.7	704.7	704.6
2	Pradola	608	606.8	607.0	607.0	606.9
3	Croveglia	601	599.8	599.8	600.3	600

2.1.5. The Mulino Delle Vene Springs

The Mulino delle Vene springs are amongst the largest springs in the Apennines, with a mean annual discharge of 96.8 L/s and a dynamic storage of $1.53 \cdot 10^6$ m^3. Hence, they can be considered the main water resources in the area [16,18,22]. These springs have been the object of comprehensive study

and analysis since 2013 [22]. In particular, the springs' discharge, the electrical conductivity, and water temperature have been monitored continuously from 11 March 2013 until 4 June 2016 at an hourly time step (Figure 4) by the regional environmental agency (Agenzia Regionale per la Prevenzione, l'Ambiente e l'Energia dell'Emilia-Romagna, ARPAE E-R).
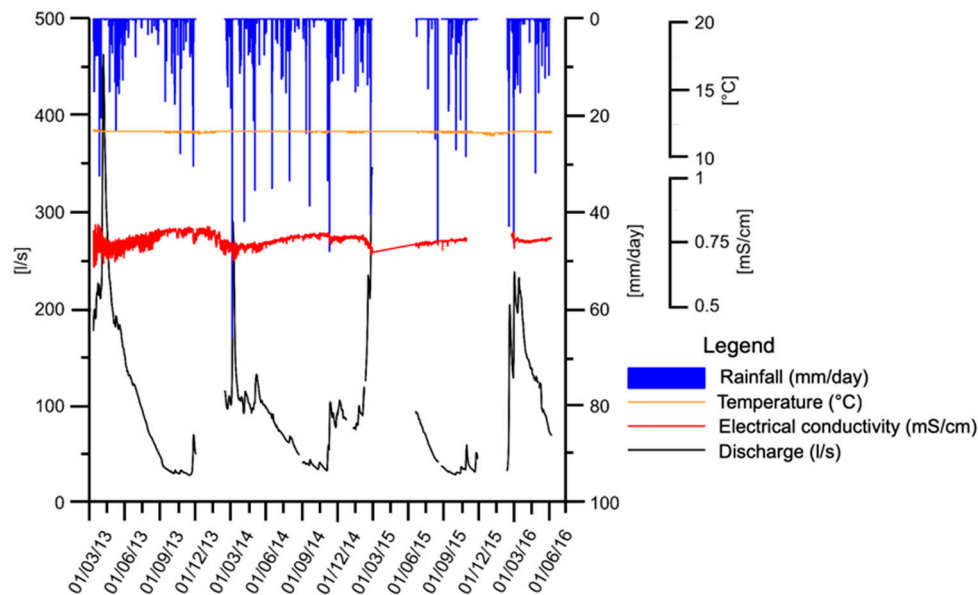

Figure 4. Hourly discharge (L/s), electrical conductivity (mS/cm), and temperature (°C) from 11 March 2013 to 4 June 2016 measured at the Mulino delle Vene springs together with daily rainfall (mm/day) at the Carpineti weather station.

The maximum average daily discharge of 462.9 L/s occurred in April 2013, while the minimum is 28.4 L/s measured in November 2013. The temperature of the water springs is constant, and it is about 12 °C. The electrical conductivity of water is strictly related to the discharge of the springs; in particular, the electrical conductivity decreases for higher discharge rates, and higher electrical conductivities are observed during low flow periods.

2.1.6. Recession Curve Analysis

Following the same method used by Cervi et al. [18], the total outflow from the springs was computed from the measured outflow in one weir, which was monitored from 2013 to 2016. Figure 4 displays the average daily discharge and the observed daily rainfall at the Carpineti weather station. The characteristic time (t_C) of the investigated aquifer, which is the needed time to reach a near-steady state after a hydraulic perturbation, was derived from the interpretation of a discharge recession curve after a rainfall period. The discharge rate evolution after a rainfall period was used to calculate the t_C of the modelled domain (PAT4). Subsequently, t_C was used to derive the storage coefficient or storativity (*S*), which is needed to undertake transient simulations. t_C was obtained from the 2013 springs recession curve because it is the longest one. The recession curve covers 226 days starting from 5 April 2013 (Q = 462.4 L/s) and ending 16 November 2013 (Q = 28.7 L/s). The analysis of the recession curve allows obtaining the depletion coefficient (*α*) that is defined as [39,40]:

$$\alpha = \frac{lnQ_0 - lnQ_t}{t},$$

(1)

where Q_0 and Q_t are the spring discharges at times 0 and t. α depends on geometrical and hydraulic properties as defined by Rorabaugh [41]:

$$\alpha = \frac{\pi^2 T}{4SL^2},\tag{2}$$

where T is the transmissivity and L is a characteristic distance of the basin. It would be possible to calculate S from Equation (2) by using the calibrated value of T with the steady state model, however, the magnitude of L is uncertain. Thus, S is indirectly derived from t_C. Assuming a linear reservoir, t_C (also named "basin constant") is defined as [42,43]:

$$t_C = \frac{SL^2}{T},\tag{3}$$

and combining Equations (2) and (3),

$$t_C = \frac{\pi^2}{4\alpha}\tag{4}$$

Once t_C is computed using Equation (4), S is obtained numerically by modifying its value in successive numerical simulations until a near-steady state after a hydraulic perturbation is reached at a time equal to t_C.

2.2. Numerical Model

2.2.1. Main Characteristics

The study area was modelled assuming an Equivalent Porous Medium (EPM) approach. This approach does not allow modelling individual fractures [44,45] and may fail when computing fast responses of single events. However, it provides information about the general behavior of the system. The EPM approach allows computing the main trends of the system and is useful to simulate the groundwater response to large-scale events such as global warming. The EPM approach was chosen based on previous studies which (1) have not identified relevant karstic features and (2) have proved its usefulness for modelling aquifers located in the Apennines [9,12]. In addition, several authors have demonstrated the efficiency of the EPM approach for modelling fractured aquifers [46,47].

The finite element code TRANSIN IV [48] with the visual interface VISUAL TRANSIN [49] was used to build a pseudo-two-dimensional numerical model consisting of one layer where the vertical dimension is implemented by multiplying the hydraulic conductivity times the aquifer thickness. This code solves the direct and inverse problems for linear and non-linear flow and transport equations. It uses linear finite elements for spatial discretization and weighted finite differences for time integration [48]. TRANSIN IV, which has been extensively used so far [50–56], allows for the simulation of groundwater flow and transport processes. TRANSIN-IV performs automatic calibration (also termed inverse problem or back analysis) using the Levenberg–Marquardt algorithm [57–59] and uses the maximum likelihood method to define the objective function.

2.2.2. Spatial Features and Zonification

The modelled domain covers an area of 5.73 km^2 and its maximum size in the North–South and West–East directions are 3.2 and 4 km, respectively. The model is delineated depending on hydrogeological and morphological features in order to be able to implement a no-flow condition along the boundary. Thus, the model boundary agrees with the limit of the PAT4 sandstones because they are surrounded by units with low values of hydraulic conductivity and water exchange between them can be neglected. The only exception is in the North-West section where a small area made up by PAT4 sandstones is excluded following the watershed because it belongs to another sub-basin. The mesh is made up by triangular elements and has 3289 nodes. The average size of the elements is, approximately, 50 m, which means that the side of the triangles is 50 m long (Figure 5). The numerical

model consists of one layer with variable thickness (Figure 5). The modelled domain is divided in four zones of different hydraulic conductivity on the basis of previous results, summarized in Sections 2.1.3 and 2.1.4, considering the geological characteristics of different materials (Section 2.1.3) and the results obtained by geo-structural field surveys performed on 19 outcrops and by pumping tests (Figure 3 and Table 1 in Section 2.1). The southern area, from the springs to the main fault along Rio Fontanello (A), appears to be fractured and, therefore, it is assumed to be relatively more permeable. The geo-structural surveys have also revealed high values of *K* in the materials located in the western part of the domain (D). A less fractured area is differentiated in the central part of PAT4 (C). Finally, the alluvial and slope deposits are considered as a different zone (B). These deposits are accumulated on the top of zone C materials. Thus, given that the model has one layer, the hydraulic parameters of the zone B will depend on both (i.e., alluvial deposits and poorly fractured materials). Additionally, the central alluvial deposits are divided in two different zones (B and B+) in some models, to improve the fitting between observed and calculated piezometric heads.
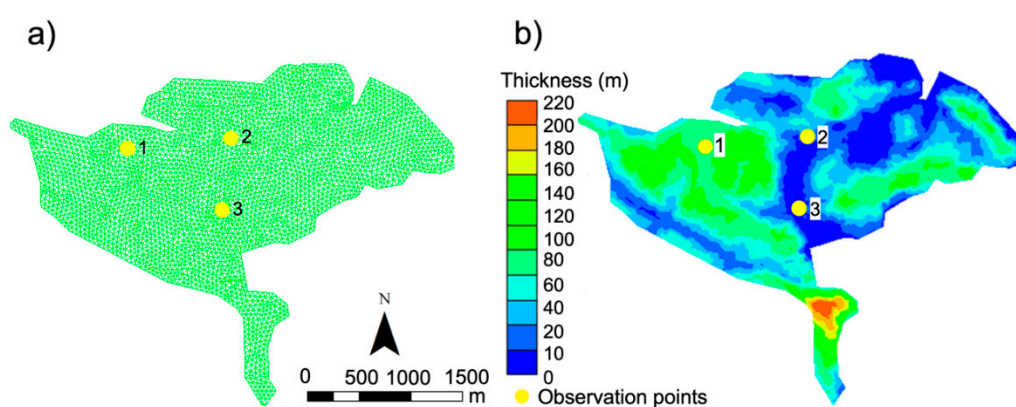

Figure 5. Spatial discretization (mesh) of the numerical model (**a**) and aquifer thickness map (**b**). The aquifer thickness allows simulating variable transmissivity through the modelled domain.

2.2.3. Boundary Conditions (BCs)

Three types of boundary conditions (BCs) were implemented in the numerical model. Springs were simulated by adopting a Dirichlet BC (prescribed head). A Neumann BC (prescribed flow) at the top of the model was used to simulate the groundwater recharge, which was assumed uniform and was computed using the Hargreaves equation. The hydrographic network was modelled by adopting a third type BC (leakage boundary) taking the topography as reference. The leakage coefficient applied to the streams was modified to simulate the real behavior of the system. In the modelled area, streams are usually dry and water exchange through them is very low (i.e., ephemeral streams). Therefore, when the piezometric head was below the surface, a low leakage coefficient was applied to constrain water exchange (water inflow). However, when the piezometric head was near or above the surface, high leakage coefficients were considered (equal or higher to the hydraulic conductivity). The hydrographic network was divided in five different zones (L1 to L5 in Figure 6) because groundwater-surface water dynamics vary along the domain. Water exchange was only constrained where and when it was needed. Interaction between groundwater and surface water through L5 requires a special definition because L5 covers a large area of the domain. If the same properties were applied to the entire L5, water would inflow and outflow through it at high and low elevations. This behavior would not agree with the nature of the system, in which only outflows at low elevations are expected. Therefore, an elevation-dependent leakage coefficient was introduced to allow water flowing out at low elevations but constraining inflows at high elevations. Finally, no-flow BCs were considered at the outer boundaries of the modelled domain because they agree with the watershed or groundwater exchange between PAT4 sandstones and surrounding clay-rich units are negligible.
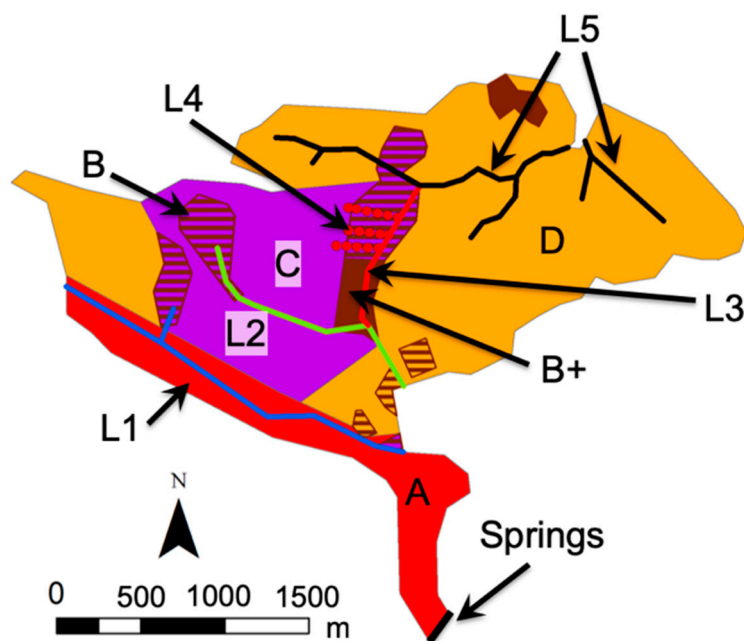
Figure 6. Zones with different hydraulic conductivity (A, B, B+, C, and D) and hydrographic network (streams) (L1, L2, L3, L4, and L5) considered in the numerical model. The hydrographic network is divided in five different zones (highlighted with different colours) because the groundwater-surface water dynamics vary along the domain.

2.2.4. Temporal Discretization

The numerical model was calibrated in steady state to compute the *K* of the different materials. Subsequently, transient simulations were undertaken to predict the behavior of the system under different scenarios of groundwater recharge. The transient model simulates a period of three years with time steps of 10 days. This period of time, which is enough to reach steady state conditions, was chosen according to t_C.

2.2.5. Calibration Strategy

The calibration process was carried out by fitting the mean piezometric head in three observation points. There were only three measurements at each observation point and all of them were taken in the same year and in the same season. Thus, a steady state calibration was undertaken because the available data were not enough for a transient calibration. The lack of data increases the uncertainty of the model, and for this reason, other kinds of observation were used to validate the calibrated model. For example, it was verified that computed spring discharge fits with the measured one. In addition, the exchange between groundwater and surface water bodies (streams) was carefully examined and only those solutions in which water exchange through ephemeral streams is very low or null were considered. Finally, it was checked that the computed groundwater level did not exceed the topography. Concerning the characteristics of the central alluvial deposits, two hypotheses were considered. Hypothesis 1 (H1) assumes that hydraulic properties of central alluvial deposits are constant, while they are divided in two zones with different values of *K* in Hypothesis 2 (H2).

2.3. Simulations under Exceptional Recharge Scenarios

The numerical model was used to predict the behavior of the system under different recharge scenarios (i.e., dry and wet scenarios), which were defined according to historical data. Analyzing historical data from the Carpineti weather station, the driest year was the 2011 with an annual rainfall amount of 544 mm, whilst the wettest year occurred in 1960 with a precipitation of 1358 mm. The mean

annual groundwater recharge for both years was computed by using the Hargreaves formula. The estimated groundwater recharge for 2011 considering an infiltration coefficient of 0.82 [39] was 351 mm, while that computed for the wettest year was 920 mm. In the case of the wettest year, the infiltration coefficient was assumed equal to the mean assessed during the years 2009–2015 because temperature data were not available.

Six different scenarios (Table 3) were simulated by varying the groundwater recharge, which was increased in three "wet" scenarios (scenarios 1 to 3 in Table 3) and decreased in three "dry" scenarios (scenarios 4 to 6 in Table 3). The driest (scenario 1) and wettest (scenario 4) scenarios were simulated implementing the minimum and maximum annual groundwater recharge recorded in the historical data. Intermediate scenarios were simulated by implementing a groundwater recharge equal to 10% (scenarios 3 and 6) and 50% (scenarios 2 and 5) of the variation between the average groundwater recharge and that observed during the driest and wettest periods. The variation of the groundwater recharge can be also expressed as a percentage with respect to the average groundwater recharge. In these cases, the groundwater recharge variations were 56%, 28%, 6%, −40%, −20%, and −4% for scenarios 1, 2, 3, 4, 5, and 6, respectively (Table 3).

Table 3. Groundwater recharge for the six simulated scenarios. The percentage of variation in the groundwater recharge refers to the average groundwater recharge (1.6 mm/d).

Scenario	Groundwater Recharge (mm/d)	Variation with Respect to the Average (%)
1 (wettest)	2.50	56
2	2.05	28
3	1.69	6
4 (driest)	0.96	−40
5	1.28	−20
6	1.54	−4

The initial conditions used in the six simulated scenarios were the same and were chosen according to the distribution of the piezometric head in steady-state conditions, obtained from the steady-state calibration.

3. Results and Discussion

3.1. Steady State Calibration

Two different hypotheses (H1 and H2), which differ in the hydraulic properties of the central alluvial deposits (zone B), were considered in the calibration. Calibrated values of *K* for both hypotheses are very similar (Table 4). The calibrated *K* in the most fractured and conductive areas (zones A and D) agree with the literature [60–62] and with the results of the hydraulic tests carried out in the outcrops (Table 1). The calibrated *K* of low conductivity units (zone C) also agrees with the result of the pumping test executed in the area (5×10^{-7} m/s). Calibrated values of *K* represent the minimum (pumping test) and the maximum (outcrop analysis) hydraulic conductivities of PAT4. Finally, calibrated *K* for zone B (alluvial deposits and poorly fractured materials) is similar to that computed for zone C and that derived from the pumping test. The relative low value of *K* computed for zone B indicates that groundwater flow in this area is mainly controlled by the poorly fractured materials. Computed and measured piezometric heads at the observation points and springs' discharge are reported in Table 5. The correlation coefficients between the computed and measured piezometric heads are 0.96 and ≈1 in H1 and H2, respectively. Computed and averaged spring discharges (8363 m³/d, period 2013–2016) differ by 0.7% and 0.3% for H1 and H2, respectively. Figure 7 displays the computed piezometric head distribution in the modelled domain for H2. Water exchange is constrained (i.e., low values of leakage coefficient) in streams L1, L2, and L3, while they are allowed in streams L4 and L5. Although a low value is adopted for the leakage coefficient in stream L3, aquifer recharge through it is 114 and

104 m³/d for H1 and H2, respectively. These values are smaller than the volume of water flowing out the domain through L4 (270 and 280 m³/d in H1 and H2, respectively). These results suggest that part of the discharged groundwater through L4 reaches the central valley and infiltrates the aquifer. Discharge through L5 is 680–690 m³/d, which is acceptable and represents the outflow during extreme rainfall periods. Simulated discharge from springs represents 90% (both hypotheses) of the total groundwater recharge. This means that only 10% of groundwater recharge flows out the aquifer through ephemeral streams. These results corroborate the observation that streams are dry throughout the year and the assumption that their interaction with groundwater is limited. Despite the fact that results obtained under both hypotheses are acceptable and that correlation coefficients are high, it is important to highlight that for hypothesis H1, the error between simulated and observed piezometric head ranges between 4 and 14 m. This error is considerably reduced in hypothesis H2, in which it is assumed that the central alluvial deposits are divided in two zones with different hydraulic properties. Although hypothesis H2 is reasonable, future studies should be aimed at identifying any differences in the central alluvial deposits and verifying if they can actually be divided in zones depending on their hydraulic parameters. This can be achieved by performing hydraulic tests, such as slug tests, in piezometers screened in the central alluvial deposits. Simulations under exceptional scenarios were undertaken adopting the hypothesis H2 because it fits the observed piezometric head better.
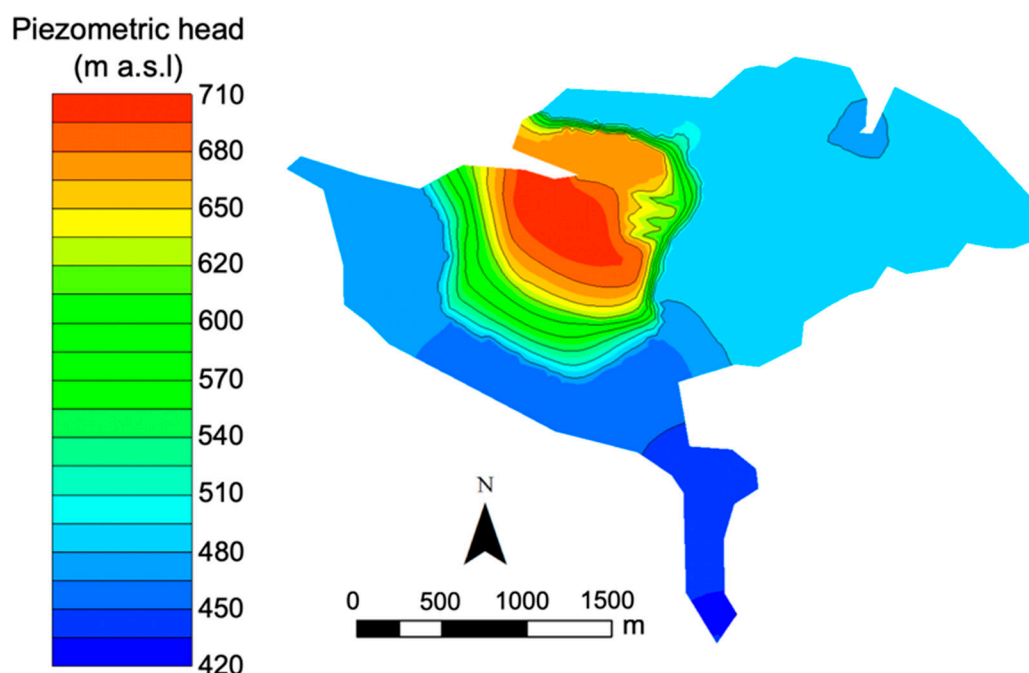

Figure 7. Piezometric head (m a.s.l.) distribution in the study area. The piezometric head distribution is computed in steady state. The head ranges between 710 (at the North side) and 420 m a.s.l. at the springs (South side).

Table 4. Calibrated values of hydraulic conductivity (*K*, m/s) for hypotheses 1 and 2 (H1 and H2).

Zone	Hypothesis 1 *K* (m/s)	Hypothesis 2 *K* (m/s)
A	2.08×10^{-4}	2.08×10^{-4}
B	1.27×10^{-6}	1.05×10^{-7}
B+	-	1.97×10^{-7}
C	1.97×10^{-7}	2.08×10^{-7}
D	2.08×10^{-4}	2.08×10^{-4}

Table 5. Measured and computed piezometric heads (m) and spring discharge (m³/d) for hypotheses H1 and H2.

Observation	Measured m a.s.l.	Hypothesis 1 m a.s.l.	Hypothesis 2 m a.s.l.
OBS1	704.6	700.8	704.6
OBS2	606.9	598.3	606.4
OBS3	600.0	614.2	599.9
Discharge (m³/d)	8363	8425	8389

3.2. Estimation of t_C and S

t_C is deduced from the spring discharge recession curve and applying Equation (4). The 2013 spring recession curve (Figure 8) was chosen for the analysis because during this period the recession curve was particularly long, and the different parts of the hydrograph can be determined. Only one recession curve was analyzed because no other recession curves as long as the one used for this study are available. Anyway, analyses of other recession curves would not have provided additional information, but they would only have been useful to corroborate the calculated parameters because, in principle, the variability of the recession slope in different recession curves of the same spring is small [63]. Thus, the same or very similar results are obtained when different recession curves of the same spring are analyzed. The recession curve shows three periods identified by three different slopes. The first part of the curve (1st period, green dashed line in Figure 8b) is the steepest one and it lasted 31 days, from 5 April 2013 to 5 May 2013. The second part of the curve (2nd period, blue dashed line in Figure 8b) is gentler and clearly visible up to the beginning of September (4th). The last part of the curve (3rd period, orange dashed line in Figure 8b) is characterized by the lowest slope and it ended on the 16 November. Depletion coefficients are 5.2×10^{-2}, 3.3×10^{-2} and 2.6×10^{-3} d^{-1} for the first, second, and third recession periods, respectively. Depletion coefficients can be attributed to different mechanisms of flow towards the springs. The first recession period accounts for the immediate response of the system to precipitation and it would be dominated by runoff and fast flow dynamics. During this period, in addition of runoff, groundwater reaching the springs would flow through large fractures and high hydraulic conductivity areas. During the second recession period, groundwater reaching the springs would flow through small fractures, and finally, during the third recession period, spring discharge would be controlled by materials that behave as a porous medium. This behavior is similar to that observed in karst systems [64]; however, in this case, water would not flow through large voids during the first period. Depletion coefficients during the first and second periods are similar, and it is assumed that the difference is related to the size of fractures through which the groundwater flows. The third depletion coefficient is the only used to derive hydraulic parameters because it would provide information concerning the porous areas within the system. Applying Equation (4) and the depletion coefficient of the third recession period, a value of ≈950 days (2.6 years) is calculated for t_C. This information is relevant for designing water management strategies because t_C allows predicting the behavior of aquifers under changes of groundwater recharge. t_C indicates the required time to reach a near-steady state after a change in the system and the capacity of the aquifer to smoothen the effects of short variations in groundwater recharge. If t_C is high, (1) the effects of short variations of groundwater recharge on the baseflow (i.e., springs' discharge) are smoothed, (2) the decrease in baseflow induced by long-lasting changes of groundwater recharge is slow, and (3) the recovery time after the cessation of an anomalous groundwater recharge period is high. The opposite behavior occurs for low values of t_C. The calculated t_C indicates that the aquifer has enough capacity to smoothen short variations of groundwater recharge. These variations would not be a constraint to use the spring discharge as an almost constant source of water. If changes of groundwater recharge last for more than 2.6 years, their effects will affect the springs' discharge. Although 2.6 years is the time to reach the near-steady state, 63% of a permanent change of groundwater recharge will be observed after ≈1/3 of t_C [65]. Thus, groundwater recharge variations longer than 10 months will noticeably affect the springs' discharge.
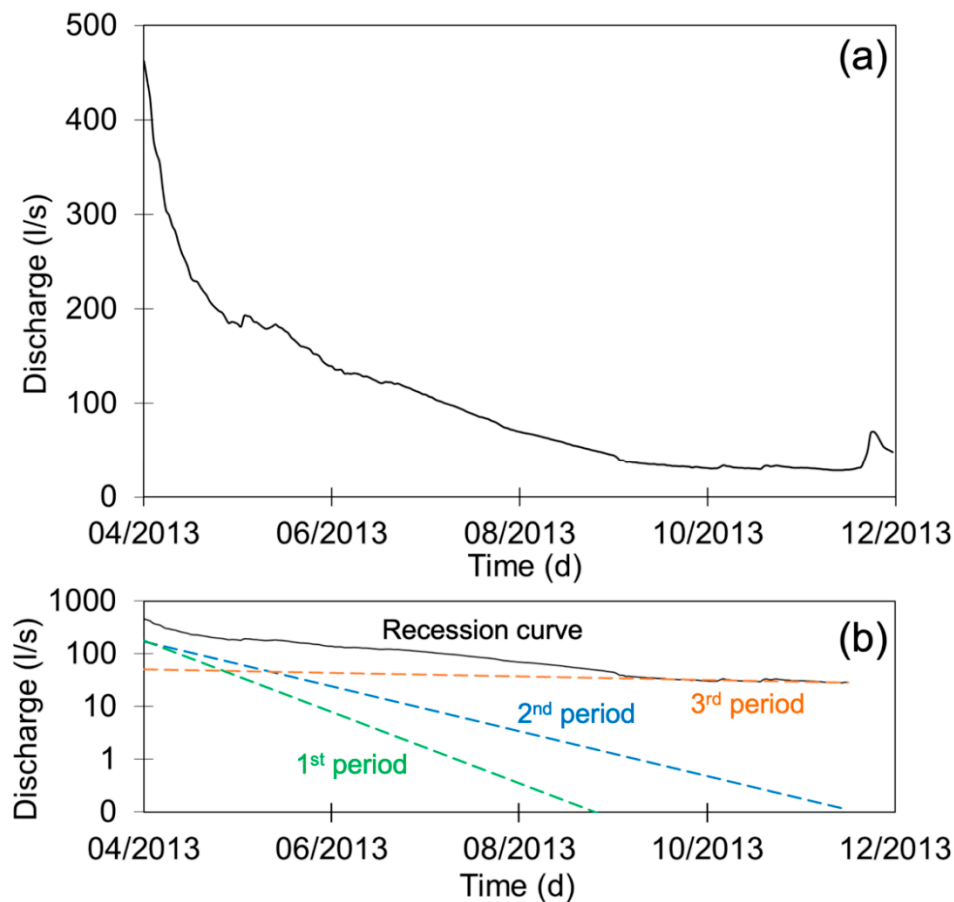
Figure 8. (**a**) Recession curve of the Mulino delle Vene springs (L/s), from 5 April 2013 to 16 November 2013. (**b**) Semi logarithmic graph of the recession curve (black line) that also includes the slope of the recession curve during the 1st period (green dashed line), the 2nd period (blue dashed line), and the 3rd period (orange dashed line).

Subsequently, *S* was calculated by using the numerical model and a trial-and-error method. Numerous transient simulations were performed varying the value of *S*, and the time to reach a near-steady state after an initial hydraulic perturbation (i.e., groundwater recharge is increased by 1 mm/d) was calculated. The selected value of *S* is that for which the steady state is reached after a time equal to t_C (i.e., 950 days). It occurs for a value of *S* equal to 0.0013. Figure 9 shows the variation of the spring discharge and the derivative of the spring discharge with respect to the logarithm of the time. The steady state is reached when the derivative of the spring discharge with respect the logarithm of the time is near 0. The calculated *S* is an effective storage coefficient and is representative of the volume of aquifer that influences the spring discharge during the assessed period. It is possible to assume that the calculated *S* is representative of the whole studied area. The value of *S* can vary at a local scale, with respect the effective one, because it depends on aquifer thickness, and, therefore, predictions on groundwater behavior at local scale may fail accordingly. However, this fact does not have relevant implications for the objectives of this work since at the aquifer scale and during long time periods the groundwater behavior is controlled by the effective *S*.

The methodology used to derive aquifer parameters from a recession curve is not a novelty. In fact, there are numerous examples in the literature in which the recession curve of springs [63,66–68] or stream baseflow [69–72] are used to infer aquifer characteristics. Recession curve interpretation is mainly used in karstic contexts, but it can be also used to characterize other types of aquifers [73]. The main difference between the methodology used in this study and that used by other authors would

be the procedure to derive *S*, which is chosen according to the time needed by the numerical model to reach the steady state after a hydraulic perturbation.
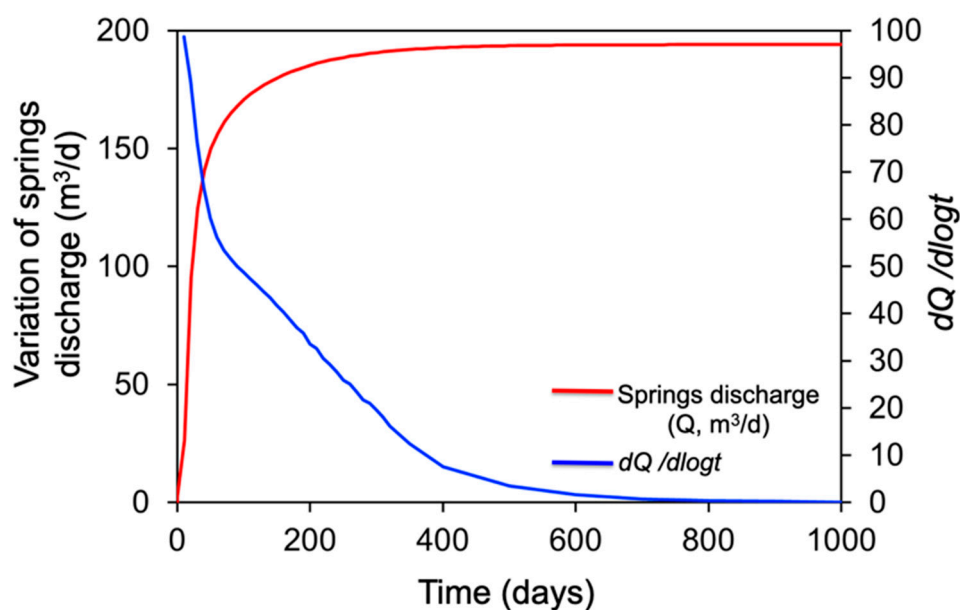

Figure 9. Variation of the spring discharge (red line) and derivative of the springs' discharge (blue line) with respect the logarithm of the time after an increase of the groundwater recharge of 1 mm/d. The steady state is reached when the derivative of the springs' discharge is 0.

3.3. Transient Simulations under Exceptional Recharge Scenarios

Six transient simulations were undertaken based on the maximum and minimum annual groundwater recharge calculated using the historical data recorded at the Carpineti weather station (Table 3). The effects of climate change on groundwater resources have been previously analyzed in numerous studies. The methodology used in most of them consist of defining the groundwater recharge scenarios based on the results of Regional Climate Models (RCM) [74–76]. This methodology may increase uncertainty [77], especially in very small areas like the one considered in this work. For this reason, the simulated scenarios were defined based on historical data recorded in a nearby weather station. For a better understanding of the results, it is important to clarify that the numerical code used to build the model simulates the aquifer as confined and calculates pressure head instead of hydraulic head. Moreover, it does not consider the unsaturated zone, and assumes constant transmissivity and horizontal groundwater flow. Although the simulated aquifer is mostly unconfined, this approach is valid for solving groundwater flow problems in most cases, especially at large scale, where aquifer thickness is much smaller than the horizontal aquifer extent. This means that the computed piezometric head under extreme conditions may be located above the surface or below the bottom of the aquifer. In these cases, the results must be carefully interpreted. If the piezometric head is above the surface, groundwater will flow out the aquifer through streams. On the contrary, the aquifer will be dried when the piezometric head is located below its bottom.

Figure 10 displays the piezometric head evolution computed for the six scenarios in the observation points 1, 2, and 3. As expected, steady state in all the scenarios is reached after 950 days. When steady state is reached, maximum piezometric head variations are computed for the observation point 1 (100 m at the extreme scenarios), while in observations points 2 and 3 they are about 50 m. Piezometric head variations decrease noticeably when the variation in groundwater recharge is lower. In observation point 1, maximum piezometric head variations are around 10 m for scenarios 3 and 6 and 50 m for scenarios 2 and 5. Although maximum piezometric head variations appear to be large, they are computed assuming that the duration of the change in groundwater recharge is long and the

steady state is finally reached. If the period during which groundwater recharge varies is shorter than the time needed to reach the steady state, piezometric heads will show less variations and will recover their average (i.e., initial) position after the cessation of the anomalous groundwater recharge period.
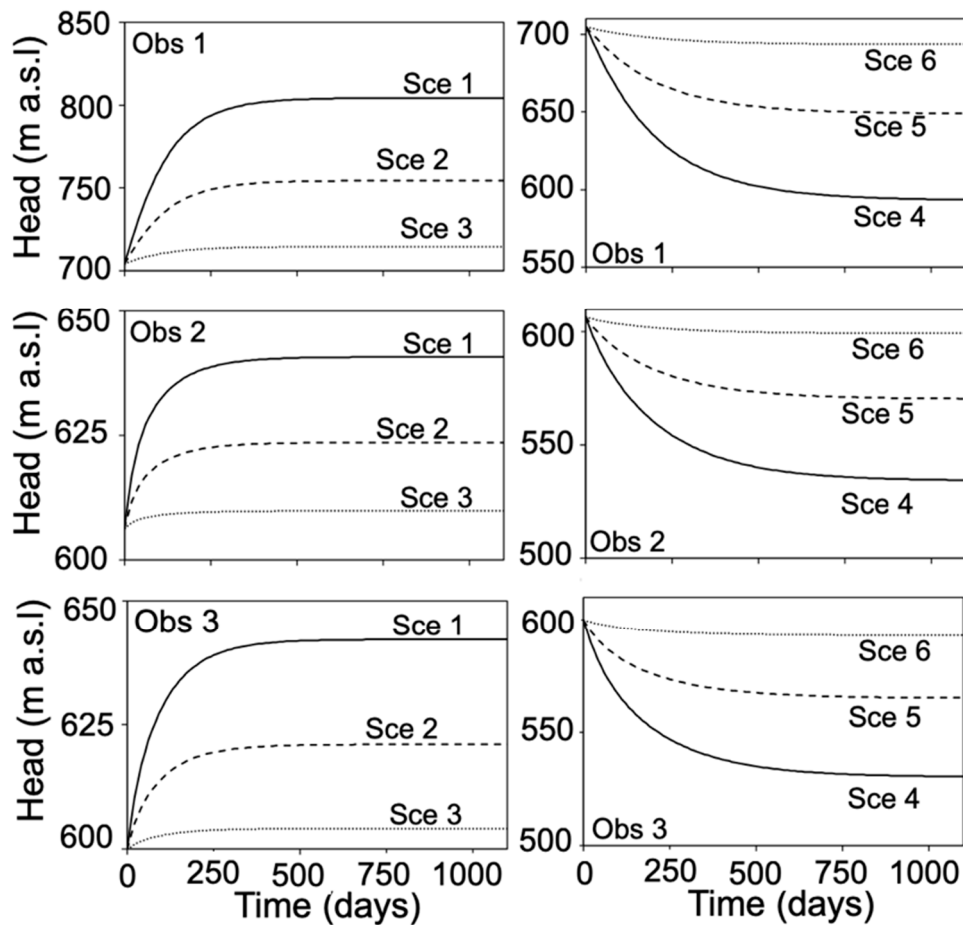

Figure 10. Piezometric head evolution (m a.s.l.) at three observation points for six simulated scenarios. Groundwater recharge is increased by 56% (Sce1), 28% (Sce2), and 6% (Sce3) in three wet scenarios (**left**) and decreased by 40% (Sce4), 20% (Sce5), and 4% (Sce6) in three dry scenarios (**right**). The percentage of variation in the groundwater recharge refers to the average groundwater recharge (1.6 mm/d).

Figure 11 displays the piezometric head variations with respect to the steady state model for the six simulated scenarios. Results are computed after a simulation period of 1 month, 6 months, and when the steady state is reached. It is possible to observe that the central zone of the domain (low *K*) is the most sensitive to variations in groundwater recharge. This means that areas with high values of hydraulic conductivity have the capacity to smoothen the effects of groundwater recharge variations. The results show that small changes in groundwater recharge (scenarios 3 and 6) produce relatively small groundwater variations, even after long simulation periods. When groundwater recharge is modified by 50% of the variation assumed in the extreme scenarios (scenarios 2 and 5), the piezometric head variations are relatively small after short time periods. However, if the change of groundwater recharge is persistent, the variations of the piezometric head will be considerable, as those observed in the extreme scenarios (scenarios 1 and 4). Although the piezometric head variations in the center of the modelled domain are high, these are relatively small in the areas with high values of hydraulic conductivity, where groundwater might be extracted. If, for example, groundwater was exploited through pumping wells, the results indicate that the wells should be constructed in the most transmissive areas and should be screened, at least, up to 25 m below the position of the

water table. This configuration would ensure that pumping wells would not fall dry in the case of long droughts or persistent reduction of groundwater recharge. Similarly, if groundwater recharge increases, the results indicate that ephemeral streams would increment their flow rate (in fact, some of them could become perennial streams). This additional water should be considered for defining water management strategies.
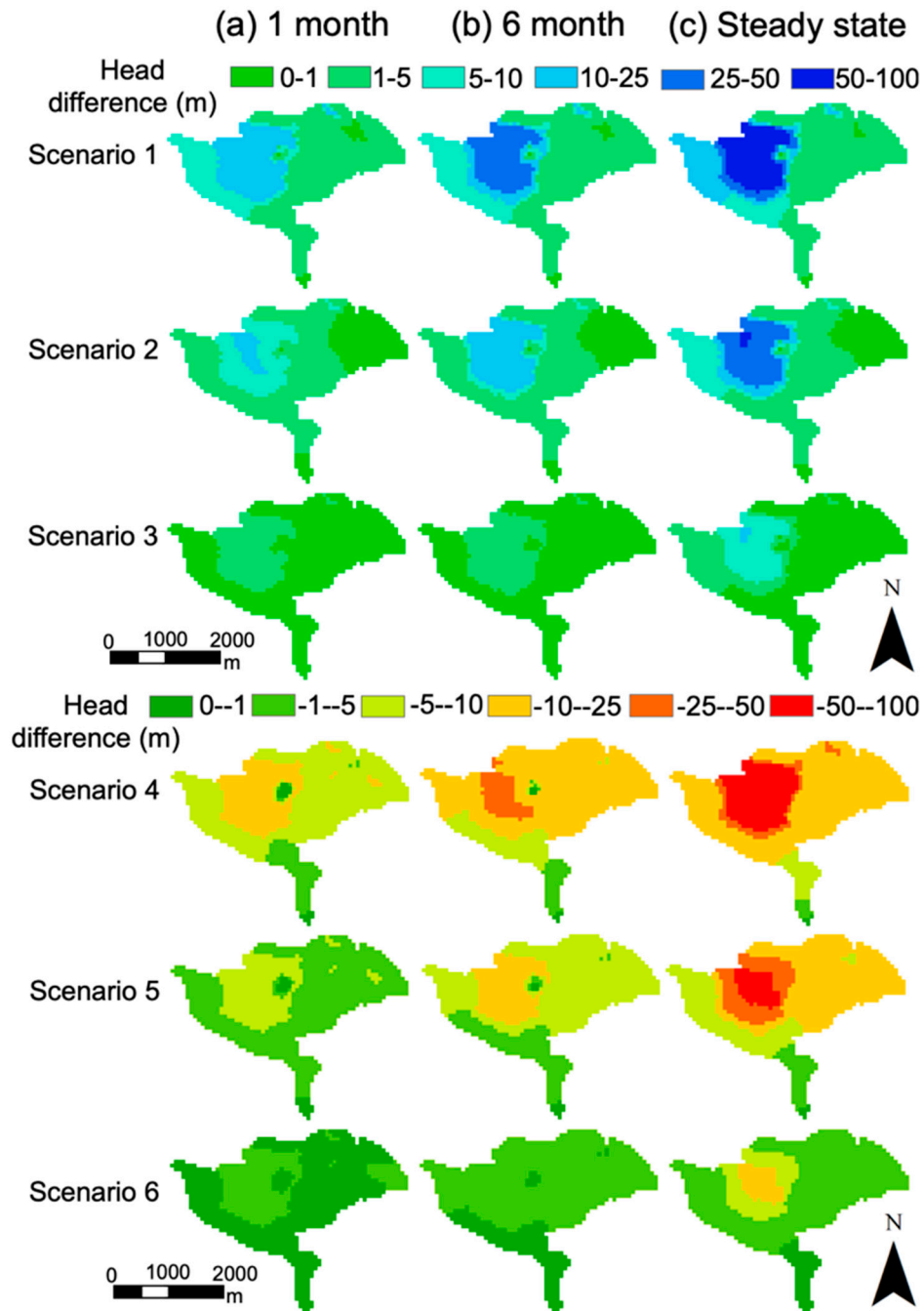
Figure 11. Piezometric head variations (m) computed for the six simulated scenarios. Results are shown after 1 (**left**) and 6 (**middle**) months of simulation and when the steady state (**right**) is reached (>950 days). Groundwater recharge is increased by 56% (Sce1), 28% (Sce2), and 6% (Sce3) in three wet scenarios and decreased by 40% (Sce4), 20% (Sce5), and 4% (Sce6) in three dry scenarios. The percentage of variation in the groundwater recharge refers to the average groundwater recharge (1.6 mm/d).

Figure 12 shows the spring discharge evolution for the six simulated scenarios. Groundwater discharge increases by 20%, 10%, and 2% in scenarios 1, 2, and 3 and decreases by 40%, 20%, and 4% for the scenarios 4, 5, and 6. As expected, the steady state is reached after 950 days of simulation. Results show that the final effects of changes in groundwater recharge are not observed immediately. The spring discharge does not show a linear relationship with groundwater recharge. In fact, the computed variations of the spring discharge are higher in the dry scenarios. This fact is a consequence of the interactions between groundwater and surface water bodies such as ephemeral streams. Groundwater outflow through ephemeral streams increases when the piezometric head rises in the wet scenarios. As a result, a portion of groundwater does not flow out the aquifer through the springs and the increase of the spring discharge is lower than that of groundwater recharge. Conversely, the changes in the spring discharge are equal to the variation of groundwater recharge in the dry scenarios because the groundwater exchange through ephemeral streams decreases when the piezometric head declines.
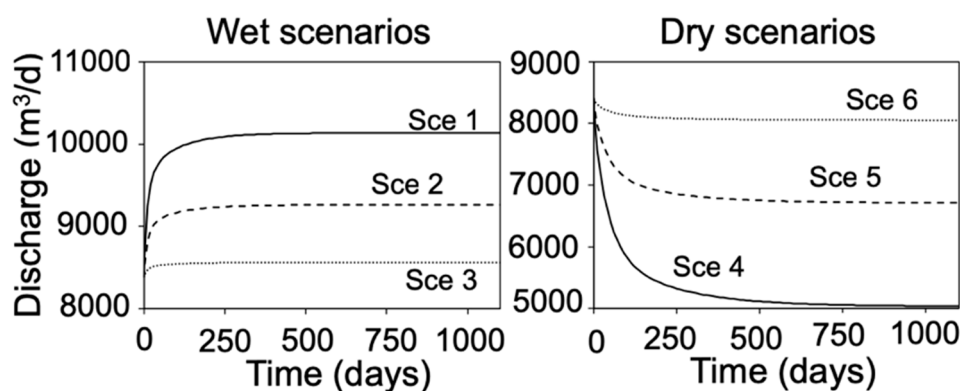

Figure 12. Spring discharge evolution (m^3/day) for the six simulated scenarios. Groundwater recharge is increased by 6% (Sce3), 28% (Sce2), and 56% (Sce1) in three wet scenarios (**left**) and decreased by 40% (Sce4), 20% (Sce5), and 4% (Sce6) in three dry scenarios (**right**). The percentage of variation in the groundwater recharge refers to the average groundwater recharge (1.6 mm/d).

3.4. Sources of Uncertainty

Main sources of modelling uncertainty may be related to hydraulic parameters, modelling inputs, conceptual model, and modelling approach. Parameter uncertainty is a consequence of the poor number of observations (only three observation points and lack of continuous record of measurements). This limitation implies that the model has to be calibrated in steady-state conditions and that the calibration results could not be sensitive to the hydraulic parameters of some areas located far from the observation points. New observation points strategically distributed and continuous measurements would contribute to reduce parameter uncertainty. Modelling input uncertainty is a consequence of the implemented groundwater recharge in the calibration and simulation stages. Groundwater recharge used for calibration was analytically calculated from data collected at a nearby weather station (Carpineti weather station). Specifically, it was calculated on a daily time scale and considering the Hargreaves formula [26] for computing the evapotranspiration. A weather station located in the modelled area would contribute to reduce uncertainty, as well as implementing the groundwater recharge calculated by other methods (analytical or numerical). The groundwater recharge used for the simulations was derived from historical data measured in the Carpineti weather station. The main source of uncertainty is a consequence of the infiltration coefficient assumed to calculate the recharge during the wettest period because temperature data are not available. There is also an uncertainty inherent to the adopted conceptual model. In general terms, the behavior of the system is well known, but some doubts may exist about the features of some geological units and the existence of water exchanges through non-identified boundaries. This source of uncertainty was addressed by developing different models in which the features of some geological formations and the boundary conditions

were modified. Among these the best results were obtained with that shown in this paper. Finally, the modelling approach uncertainty is consequence of modelling the fractured aquifer using an EPM approach and assuming constant transmissivity and horizontal flow. The feasibility of the EPM approach for modelling fractured aquifers has been proved by numerous authors [46,47], especially at large and intermediate scales. However, this approach may fail when evaluating the groundwater behavior at local scale. Assumptions of constant transmissivity and horizontal flow are valid for solving groundwater flow problems in most cases, especially at large scale where aquifer thickness can be neglected by comparison with the horizontal aquifer extent. In this case, local results as well as those obtained after a drastic reduction of the piezometric head must be carefully analyzed.

4. Conclusions

This study represents an attempt to build a numerical model of the Mulino delle Vene fractured aquifer using an open source code. This area has been object of studies since 2013, when the springs at the outlet of the aquifer have been equipped with a monitoring system operating continuously and the hydraulic conductivity of the outcropping geological units have been assessed [19]. The hydrogeological system dynamics have been previously evaluated by Cervi et al. [18] and Vizzi [33]. The authors have identified the aquifer feeding the springs with a sandstone plateau (Pantano sandstones, sub-unit of Santa Maria, PAT4), which is crossed by a network of faults and fractures. The springs are the only water outflow of the hydrogeological structure. Unfortunately, there is little information about the piezometric head evolution and the flow paths in the fractured rock mass. However, this study shed light on the groundwater flow behavior in the aquifer. This study also shows the importance of following a proper methodology to compute groundwater recharge. In particular, realistic results were obtained by using the Hargreaves formula.

The methodology adopted to build a representative numerical model when sufficient piezometric data are not available was presented. At first, the steady state model was calibrated using the average piezometric head of two wells and one small lake, the average spring discharge, and observations on the interactions between surface water and groundwater. This calibration allows for obtaining the values of K for the different materials. Afterwards, an alternative method, which is based on the analysis of the spring discharge curve, was adopted to derive the values of S and t_C. S is essential to perform transient simulations and ascertain the behavior of the system under different groundwater recharge scenarios. t_C, in addition to allow calculating S, provides meaningful information about the behavior of the aquifer that can be used for water management purposes. A high t_C indicates that the aquifer has the capacity to smoothen groundwater recharge changes in the spring discharge, while the changes occur abruptly when t_C is low. In addition, under long-term changes in groundwater recharge, the spring discharge will evolve more slowly with higher t_C. The computed t_C is smaller than that of large and deep aquifers but it appears to be sufficient to mitigate short drought periods. Therefore, seasonal or short-term variations will not noticeably alter the springs' discharge, which could be exploited without adopting alternative measures. However, long dry periods (more than 10 months, although a steady state is reached after 2.6 years) will markedly affect the springs' discharge. Regardless, even considering the worst scenario, the springs' discharge will not be affected too much. Probably, the best option to be implemented in future water management strategies would be to limit the maximum use of spring water to the minimum flow rate computed for the worst scenario. In this case, the activities depending on spring discharge would not be affected by long drought periods.

Six transient simulations over a period of three years were undertaken to analyze the system behavior. Groundwater recharge was calculated in six scenarios according to the maximum and minimum groundwater recharge calculated using historical data. The scenarios cover a wide range of possible changes of groundwater recharge. Results indicate that under small changes of groundwater recharge with respect to extreme scenarios, the variations of the piezometric head and the spring discharge will be relatively small. On the contrary, if the variations are moderate, changes in the piezometric head and spring discharge will be considerable after some months. These numerical

results might be useful for improving groundwater management strategies in the area designing infrastructures under realistic circumstances in the context of climate change.

Local stakeholders could benefit from this research since most mountain aquifers have not been studied in detail up to now. With the aim of reducing the uncertainties in water supply during the most critical months, stakeholders in charge of water management are at the moment increasing the size of tanks and constructing artificial reservoirs to collect water from springs during the night and store it. Especially during the low-flow period, this ensures that the water needed during the day is available, if water consumption exceeds the springs' mean discharge flow. Considering the fact that the Mulino delle Vene springs are not exploited at the moment, they could become a valuable resource to overcome future water scarcity periods as those that occurred in the area during summer and the withdrawal could be regulated based on the results of this study.

References

1. Kundzewick, Z.W.; Döll, P. Will groundwater ease freshwater stress under climate change? *Hydrol. Sci. J.* **2009**, *54*, 665–675. [CrossRef]

2. IPCC. *Climate Change 2007: The Physical Science Basis. Contribution of Working Group I to the Fourth Assessment Report of the Intergovernmental Panel on Climate Change*; Solomon, S., Qin, D., Manning, M., Chen, Z., Marquis, M., Averyt, K.B., Tignor, M., Miller, H.L., Eds.; Cambridge University Press: Cambridge, UK; New York, NY, USA, 2007; p. 996.

3. IPCC. *Climate Change 2014: Synthesis Report. Contribution of Working Groups I, II and III to the Fifth Assessment Report of the Intergovernmental Panel on Climate Change*; Pachauri, R.K., Meyer, L.A., Eds.; IPCC: Geneva, Switzerland, 2014; p. 151.

4. Taylor, R.G.; Scanlon, B.; Döll, P.; Rodell, M.; Van Beek, R.; Wada, Y.; Konikow, L. Ground water and climate change. *Nat. Clim. Chang.* **2013**, *3*, 322–329. [CrossRef]

5. Dragoni, W.; Sukhija, B.S. Climate Change and Groundwater: A Short Review. In *Climate Change and Groundwater*; Dragoni, W., Sukhija, B.S., Eds.; The Geological Society of London: London, UK, 2008; Volume 288, pp. 1–12.

6. Garnier, M.; Harper, D.M.; Blaskovicova, L.; Hancz, G.; Janauer, G.A.; Jolánkai, Z.; Lanz, E.; Lo Porto, A.; Mándoki, M.; Pataki, B.; et al. Climate Change and European Water Bodies, a Review of Existing Gaps and Future Research Needs: Findings of the ClimateWater Project. *Environ. Manag.* **2015**, *56*, 271–285. [CrossRef] [PubMed]

7. ISTAT Statistiche Focus Giornata Mondiale Dell'acqua: Le Statistiche Dell'istat. Available online: https://www.istat.it/it/archivio/57514 (accessed on 14 October 2019).

8. Ducci, D.; Rusi, S.; Alberti, L.; Cerutti, P.; Fabbri, P.; Gargini, A.; La Vigna, F.; Masetti, M.; Petitta, M.; Piscopo, V.; et al. Aquifers: the natural response to the hydric emergency. *Acque Sotter. Ital. J. Groundw.* **2017**, *6*, 63.

9. Cambi, C.; Dragoni, W. Groundwater yield, climatic changes and recharge variability: Considerations out of the modelling of a spring in the Umbria-Marche Apennines. *Hydrogeologie* **2000**, *4*, 11–25.

10. Dragoni, W.; Giontella, C.; Melillo, M.; Cambi, C.; Di Matteo, L.; Valigi, D. Possible Response of Two Water Systems in Central Italy to Climatic Changes. In *Advances in Watershed Hydrology*; Moramarco, T., Barbetta, S., Brocca, L., Eds.; Water Resources Publications: Highhlands Ranch, CO, USA, 2015; pp. 397–424.

11. Gattinoni, P.; Francani, V. Depletion risk assessment of the Nossana Spring (Bergamo, Italy) based on the stochastic modeling of recharge. *Hydrogeol. J.* **2010**, *18*, 325–337. [CrossRef]

12. Dragoni, W.; Mottola, A.; Cambi, C. Modeling the effects of pumping wells in spring management: The case of Scirca spring (central Apennines, Italy). *J. Hydrol.* **2013**, *493*, 115–123. [CrossRef]

13. Liuzzo, L.; Noto, L.V.; Arnone, E.; Caracciolo, D.; La Loggia, G. Modifications in Water Resources Availability Under Climate Changes: A Case Study in a Sicilian Basin. *Water Resour Manag.* **2015**, *29*, 1117–1135. [CrossRef]

14. Vezzoli, R.; Mercogliano, P.; Pecora, S.; Zollo, A.L.; Cacciamani, C. Hydrological simulation of Po River (North Italy) discharge under climate change scenarios using the RCM COSMO-CLM. *Sci. Total Environ.* **2015**, *521–522*, 346–358. [CrossRef]

15. Morari, F.; Lugato, E.; Borin, M. An integrated non-point source model-GIS system for selecting criteria of best management practices in the Po Valley, North Italy. *Agric. Ecosyst. Environ.* **2004**, *102*, 247–262. [CrossRef]

16. Petronici, F. Impacts of Climate Change on Groundwater: Numerical Modelling of a Northern Apennines Catchment. Ph.D. Thesis, University of Bologna, Bologna, Italy, 2018.

17. Cervi, F.; Corsini, A.; Doveri, M.; Mussi, M.; Ronchetti, F.; Tazioli, A. Characterizing the Recharge of Fractured Aquifers: A Case Study in a Flysch Rock Mass of the Northern Apennines (Italy). In *Engineering Geology for Society and Territory—Volume 3*; Lollino, G., Arattano, M., Rinaldi, M., Giustolisi, O., Marechal, J.-C., Grant, G.E., Eds.; Springer International Publishing: Cham, Switzerland, 2015; pp. 563–567.

18. Cervi, F.; Marcaccio, M.; Petronici, F.; Borgatti, L. Hydrogeological characterization of peculiar Apenninic springs. In Proceedings of the International Association of Hydrological Sciences, Bologna, Italy, 4–6 June 2014; Volume 364, pp. 333–338.

19. Petronici, F. Modellazione Idrogeologica Di Un Acquifero Fratturato. Master's Thesis, University of Bologna, Bologna, Italy, 2014.

20. ISTAT Statistiche Istat. Available online: http://dati.istat.it/ (accessed on 15 October 2019).

21. Regione Emilia-Romagna. DGR 1781/2015-Aggiornamento del quadro conoscitivo di riferimento (carichi inquinanti, bilanci idrici e stato delle acque) ai fini del riesame dei Piani di Gestione Distrettuali 2015-2021—Italiano. Available online: http://ambiente.regione.emilia-romagna.it/it/acque/approfondimenti/documenti/aggiornamento-del-quadro-conoscitivo-di-riferimento-carichi-inquinanti-bilanci-idrici-e-stato-delle-acque-ai-fini-del-riesame-dei-piani-di-gestione-distrettuali-2015-2021 (accessed on 15 October 2019).

22. Cervi, F.; Petronici, F.; Castellarin, A.; Marcaccio, M.; Bertolini, A.; Borgatti, L. Climate-change potential effects on the hydrological regime of freshwater springs in the Italian Northern Apennines. *Sci. Total Environ.* **2018**, *622–623*, 337–348. [CrossRef] [PubMed]

23. Antolini, G.; Auteri, L.; Pavan, V.; Tomei, F.; Tomozeiu, R.; Marletto, V. A daily high-resolution gridded climatic data set for Emilia-Romagna, Italy, during 1961–2010. *Int. J. Climatol.* **2016**, *36*, 1970–1986. [CrossRef]

24. Tomozeiu, R.; Agrillo, G.; Cacciamani, C.; Pavan, V. Statistically downscaled climate change projections of surface temperature over Northern Italy for the periods 2021–2050 and 2070–2099. *Nat. Hazards* **2014**, *72*, 143–168. [CrossRef]

25. Dubrovský, M.; Hayes, M.; Duce, P.; Trnka, M.; Svoboda, M.; Zara, P. Multi-GCM projections of future drought and climate variability indicators for the Mediterranean region. *Reg. Environ. Chang.* **2014**, *14*, 1907–1919. [CrossRef]

26. Hargreaves, G.H.; Samani, Z.A. Reference Crop Evapotranspiration from Temperature. *Appl. Eng. Agric.* **1985**, *1*, 96–99. [CrossRef]

27. Allen, R.G.; Pereira, L.S.; Raes, D.; Smith, M. Crop evapotranspiration—Guidelines for computing crop water requirements. *Food and Agric. Organ. of the United Nations* **1998**, *56*, 15.

28. Scozzafava, M.; Tallini, M. Net infiltration in the Gran Sasso Massif of central Italy using the Thornthwaite water budget and curve-number method. *Hydrogeol. J.* **2001**, *9*, 461–475. [CrossRef]

29. Di Matteo, L.; Dragoni, W. Climate change and water resources in limestone and mountain areas: The case of Firenzuola Lake (Umbria, Italy). In Proceedings of the 8th Conference on Limestone Hydrogeology, Neuchatel, Switzerland, 21–23 September 2006; pp. 21–23.

30. Allocca, V.; Manna, F.; De Vita, P. Estimating annual groundwater recharge coefficient for karst aquifers of the southern Apennines (Italy). *Hydrol. Earth Syst. Sci.* **2014**, *18*, 803–817. [CrossRef]

31. Thornthwaite, C.W.; Charles, W.; Mather, J.R. *Instructions and Tables for Computing Potential Evapotranspiration and the Water Balance*; Laboratory of Climatology: Centerton, AR, USA, 1957.

32. Papani, G.; De NArdo, M.T.; Bettelli, G.; Rio, D.; Tellini, C.; Vernia, L. *Note Illustrative Della Carta Geologica D'italia Alla Scala 1:50.000, Foglio 218*; Servizio Geologico d'Italia—Regione Emilia Romagna: Firenze, Italy, 2002.

33. Vizzi, L. Studio Idrogeologico Delle Sorgenti Di Mulino Delle Vene. Master's Thesis, Università degli studi di Modena e Reggio Emilia, Modena, Italy, 2014.

34. Civita, M. *Idrogeologia Applicata e Ambientale*; CEA: Milano, Italy, 2005; ISBN 978-88-08-08741-6.

35. Caine, J.S.; Tomusiak, S.R.A. Brittle structures and their role in controlling porosity and permeability in a complex Precambrian crystalline-rock aquifer system in the Colorado Rocky Mountain Front Range. *GSA Bull.* **2003**, *115*, 1410–1424. [CrossRef]

36. Snow, D.T. Rock Fracture Spacings, Openings, and Porosities. *J. Soil Mech. Found. Div.* **1968**, *94*, 73–92.

37. Francani, V.; Gattinoni, P.; Scesi, L.T.G. Tensore di permeabilità e direzione di flusso preferenziale in un ammasso roccioso fratturato. *Quaderni di Geologia Applicata* **2005**, *1*, 79–98.

38. Scesi, L.; Gattinoni, P. *La Circolazione Idrica Negli Ammassi Rocciosi*; CEA: Milano, Italy, 2007; ISBN 978-88-408-1388-2.

39. Kovács, A.; Perrochet, P. A quantitative approach to spring hydrograph decomposition. *J. Hydrol.* **2008**, *352*, 16–29. [CrossRef]

40. Angelini, P.; Dragoni, W. The Problem of Modeling Limestone Springs: The Case of Bagnara (North Apennines, Italy). *Groundwater* **1997**, *35*, 612–618. [CrossRef]

41. Rorabough, M.I. Estimating changes in bank storage and grounwater contribution to streamflow. *IAHS* **1964**, *63*, 432–441.

42. Rorabaugh, M.I.; Simons, W.D. *Exploration of Methods of Relating Ground Water to Surface Water, Columbia River Basin—Second Phase*; Open-File Report; USGS: Reston, VA, USA, 1966.

43. Rorabaugh, M.I.; Simons, W.D.; Garret, A.A.; McMurtrey, R.G. *Exploration of Methods of Relating Ground-Water to Surface Water, Columbia River Basin—First Phase, with a Section on Direct Computation of Ground-Water Outflow by Electric Analogy by B.J. Bernes*; Open-File Report; USGS: Reston, VA, USA, 1966.

44. Shapiro, A.; Andersson, J. Steady state fluid response in fractured rock: A boundary element solution for a coupled, discrete fracture continuum model. *Water Resour. Res.* **1983**, *19*, 959–969. [CrossRef]

45. Teutsch, G.; Sauter, M. Groundwater modeling in karst terranes: Scale effects, data acquisition and field validation. In Proceedings of the 3rd Conference on Hydrology, Ecology, Monitoring and Management of Ground Water in Karst Terranes, Nashville, TN, USA, 4–6 December 1991; pp. 17–34.

46. Scanlon, B.R.; Mace, R.E.; Barrett, M.E.; Smith, B. Can we simulate regional groundwater flow in a karst system using equivalent porous media models? Case study, Barton Springs Edwards aquifer, USA. *J. Hydrol.* **2003**, *276*, 137–158. [CrossRef]

47. Hassan, S.M.T.; Lubczynski, M.W.; Niswonger, R.G.; Su, Z. Surface–groundwater interactions in hard rocks in Sardon Catchment of western Spain: An integrated modeling approach. *J. Hydrol.* **2014**, *517*, 390–410. [CrossRef]

48. Medina, A.; Alcolea, A.; Carrera, J.; Castro, L.F. Modelos de flujo y transporte en la geosfera: Código TRANSIN IV. (Flow and transport modelling in the geosphere: The code TRANSIN IV). In *IV Jornadas de Investigación y Desarrollo Tecnológico de Gestión de Residuos Redioactivos*; ENRESA: Barcelona, Spain, November 2000; Volume 3, pp. 195–204.

49. UPC-CSIC. *Visual Transin*; UPC-CSIC: Barcelona, Spain, 2003.

50. Medina, A.; Carrera, J. Coupled estimation of flow and solute transport parameters. *Water Resour. Res.* **1996**, *32*, 3063–3076. [CrossRef]

51. Iribar, V.; Carrera, J.; Custodio, E.; Medina, A. Inverse modelling of seawater intrusion in the Llobregat delta deep aquifer. *J. Hydrol.* **1997**, *198*, 226–244. [CrossRef]

52. Medina, A.; Carrera, J. Geostatistical inversion of coupled problems: Dealing with computational burden and different types of data. *J. Hydrol.* **2003**, *281*, 251–264. [CrossRef]

53. Font-Capo, J.; Pujades, E.; Vàzquez-Suñé, E.; Carrera, J.; Velasco, V.; Montfort, D. Assessment of the barrier effect caused by underground constructions on porous aquifers with low hydraulic gradient: A case study of the metro construction in Barcelona, Spain. *Eng. Geol.* **2015**, *196*, 238–250. [CrossRef]

54. Culí, L.; Pujades, E.; Vázquez-Suñé, E.; Jurado, A. Modelling of the EPB TBM shield tunnelling advance as a tool for geological characterization. *Tunn. Undergr. Space Technol.* **2016**, *56*, 12–21. [CrossRef]

55. Jurado, A.; Vázquez-Suñé, E.; Pujades, E. Potential uses of pumped urban groundwater: A case study in Sant Adrià del Besòs (Spain). *Hydrogeol. J.* **2017**, *25*, 1745–1758. [CrossRef]

56. Serrano-Juan, A.; Pujades, E.; Vázquez-Suñè, E.; Velasco, V.; Criollo, R.; Jurado, A. Integration of groundwater by-pass facilities in the bottom slab design for large underground structures. *Tunn. Undergr. Space Technol.* **2018**, *71*, 231–243. [CrossRef]

57. Carrera, J.; Neuman, S.P. Estimation of Aquifer Parameters Under Transient and Steady State Conditions: 1. Maximum Likelihood Method Incorporating Prior Information. *Water Resour. Res.* **1986**, *22*, 199–210. [CrossRef]

58. Carrera, J.; Neuman, S.P. Estimation of Aquifer Parameters Under Transient and Steady State Conditions: 2. Uniqueness, Stability, and Solution Algorithms. *Water Resour. Res.* **1986**, *22*, 211–227. [CrossRef]

59. Carrera, J.; Neuman, S.P. Estimation of Aquifer Parameters Under Transient and Steady State Conditions: 3. Application to Synthetic and Field Data. *Water Resour. Res.* **1986**, *22*, 228–242. [CrossRef]

60. Allen, D.J.; Brewerton, L.J.; Coleby, L.M.; Gibbs, B.R.; Lewis, M.A.; MacDonald, A.M.; Wagstaff, S.J.; Williams, A.T. *The Physical Properties of Major Aquifers in England and Wales*; British Geological Survey Technical Report WD/97/34: Nottingham, UK, 1997; p. 312.

61. Gómez, A.A.; Rodríguez, L.B.; Vives, L.S. The Guarani Aquifer System: Estimation of recharge along the Uruguay–Brazil border. *Hydrogeol. J.* **2010**, *18*, 1667–1684. [CrossRef]

62. Zhang, H.; Hiscock, K.M. Modelling the impact of forest cover on groundwater resources: A case study of the Sherwood Sandstone aquifer in the East Midlands, UK. *J. Hydrol.* **2010**, *392*, 136–149. [CrossRef]

63. Amit, H.; Lyakhovsky, V.; Katz, A.; Starinsky, A.; Burg, A. Interpretation of Spring Recession Curves. *Groundwater* **2002**, *40*, 543–551. [CrossRef]

64. Ghasemizadeh, R.; Hellweger, F.; Butscher, C.; Padilla, I.; Vesper, D.; Field, M.; Alshawabkeh, A. Review: Groundwater flow and transport modeling of karst aquifers, with particular reference to the North Coast Limestone aquifer system of Puerto Rico. *Hydrogeol. J.* **2012**, *20*, 1441–1461. [CrossRef] [PubMed]

65. Ponce, V.M.; Kumar, S.; Aguilar, R.D. Regional Aquifer Parameters Using Baseflow Recession. Available online: http://ponce.sdsu.edu/regional_aquifer_parameters.html (accessed on 15 October 2019).

66. Fatchurohman, H.; Adji, T.N.; Haryono, E.; Wijayanti, P. Baseflow index assessment and master recession curve analysis for karst water management in Kakap Spring, Gunung Sewu. *IOP Conf. Ser. Earth Environ. Sci.* **2018**, *148*, 012029. [CrossRef]

67. Shamsi, A.; Karami, G.H.; Taheri, A. Recession curve analysis of major karstic springs at the Lasem area (north of Iran). *Carbonates Evaporites* **2019**, *34*, 845–856. [CrossRef]

68. Płaczkowska, E.; Siwek, J.; Maciejczyk, K.; Mostowik, K.; Murawska, M.; Rzonca, B. Groundwater capacity of a flysch-type aquifer feeding springs in the Outer Eastern Carpathians (Poland). *Hydrol. Res.* **2018**, *49*, 1946–1959. [CrossRef]

69. Oyarzún, R.; Godoy, R.; Núñez, J.; Fairley, J.P.; Oyarzún, J.; Maturana, H.; Freixas, G. Recession flow analysis as a suitable tool for hydrogeological parameter determination in steep, arid basins. *J. Arid Environ.* **2014**, *105*, 1–11. [CrossRef]

70. Pauritsch, M.; Birk, S.; Wagner, T.; Hergarten, S.; Winkler, G. Analytical approximations of discharge recessions for steeply sloping aquifers in alpine catchments. *Water Resour. Res.* **2015**, *51*, 8729–8740. [CrossRef]

71. Sánchez-Murillo, R.; Brooks, E.S.; Elliot, W.J.; Gazel, E.; Boll, J. Baseflow recession analysis in the inland Pacific Northwest of the United States. *Hydrogeol. J.* **2015**, *23*, 287–303. [CrossRef]

72. Huang, C.-C.; Yeh, H.-F. Hydrogeological Parameter Determination in the Southern Catchments of Taiwan by Flow Recession Method. *Water* **2019**, *11*, 7. [CrossRef]

73. Jakada, H.; Chen, Z.; Luo, M.; Zhou, H.; Wang, Z.; Habib, M. Watershed Characterization and Hydrograph Recession Analysis: A Comparative Look at a Karst vs. Non-Karst Watershed and Implications for Groundwater Resources in Gaolan River Basin, Southern China. *Water* **2019**, *11*, 743. [CrossRef]

74. Goderniaux, P.; Brouyère, S.; Fowler, H.J.; Blenkinsop, S.; Therrien, R.; Orban, P.; Dassargues, A. Large scale surface–subsurface hydrological model to assess climate change impacts on groundwater reserves. *J. Hydrol.* **2009**, *373*, 122–138. [CrossRef]

75. van Roosmalen, L.; Sonnenborg, T.O.; Jensen, K.H.; Christensen, J.H. Comparison of Hydrological Simulations of Climate Change Using Perturbation of Observations and Distribution-Based ScalingAll rights reserved. No part of this periodical may be reproduced or transmitted in any form or by any means, electronic or mechanical, including photocopying, recording, or any information storage and retrieval system, without permission in writing from the publisher. *Vadose Zone J.* **2011**, *10*, 136–150.

76. Pulido-Velazquez, D.; García-Aróstegui, J.L.; Molina, J.-L.; Pulido-Velazquez, M. Assessment of future groundwater recharge in semi-arid regions under climate change scenarios (Serral-Salinas aquifer, SE Spain). Could increased rainfall variability increase the recharge rate? *Hydrol. Process.* **2015**, *29*, 828–844. [CrossRef]

77. Kurylyk, B.L.; MacQuarrie, K.T.B. The uncertainty associated with estimating future groundwater recharge: A summary of recent research and an example from a small unconfined aquifer in a northern humid-continental climate. *J. Hydrol.* **2013**, *492*, 244–253. [CrossRef]